https://doi.org/10.64504/big.dv3i1.326

Adhesive Force of a Single Boston Ivy Adhesive Disc: Quantitative Biomechanical Analysis and Comparison with Gecko Adhesion

1st Zhenyu Liu
College of Computer Science and Technology
Zhejiang University
Hangzhou, China
liuzhenyu0713@zju.edu.cn

2nd Huajian Xiao *
Guangzhou Songyin Electronic Technology Co., Ltd.
Guangzhou, China
18428353004@163.com

Received on September 6th, revised on October 21st, accepted on November 12th, published on January 6th.

Abstract*—Climbing plants represent a remarkable example of biological engineering, having evolved diverse mechanisms for vertical ascent and permanent attachment to substrates. Boston ivy (Parthenocissus tricuspidata), a member of the Vitaceae family, achieves exceptional adhesive strength through specialized disc-shaped structures at the termini of its tendrils. Despite extensive morphological studies dating back to Darwin's observations in the 19th century, quantitative biomechanical characterization of individual adhesive discs has remained elusive. Here, we present the first direct measurements of the adhesive force generated by a single Boston ivy disc using a custom-fabricated micro-electromechanical system (MEMS) force sensor with nanonewton resolution. Our measurements reveal that a single disc, with an average contact area of 1.22 ± 0.3 mm² and mass of 0.5 ± 0.1 mg, generates an extraordinary adhesive force of 13.7 ± 2.1 N (mean ± s.d., n=25), corresponding to an adhesive stress of approximately 11.2 N/mm². This represents a force-to-weight ratio exceeding 27,000:1, making it one of the strongest biological adhesives known. Comparative analysis demonstrates that the adhesive stress of Boston ivy is more than two orders of magnitude greater than that of gecko setae (0.1 N/mm²). Through enzymatic degradation experiments, we demonstrate that the adhesion is primarily mediated by secreted polysaccharide-based adhesive compounds, with mechanical interlocking playing a secondary role. The adhesive force exhibits a strong linear correlation with perpendicular preload force ($R^2 = 0.89$, $p < 0.001$), suggesting that contact area and adhesive spreading are critical determinants of bond strength. Scanning electron microscopy (SEM) and atomic force microscopy (AFM) reveal a complex hierarchical structure featuring micro-channels that facilitate adhesive secretion and distribution. Chemical analysis via high-performance liquid chromatography-mass spectrometry (HPLC-MS) identifies the adhesive as primarily composed of debranched rhamnogalacturonan I polysaccharides with molecular weights ranging from 50-200 kDa. These findings challenge the paradigm that van der Waals forces dominate biological adhesion and provide a blueprint for developing high-strength, permanent, wet-tolerant bio-inspired adhesives for applications in construction, marine engineering, and biomedical devices.

Keywords*—Parthenocissus tricuspidata, adhesive disc, biological adhesion, polysaccharide adhesive, biomechanics, MEMS force sensor, climbing plants, bio-inspired materials

1. Introduction

1.1. Background and Motivation

The ability of organisms to adhere to surfaces is fundamental to survival, enabling locomotion, feeding, and long-term occupation of diverse ecological niches [1,2]. Across biological systems, adhesion strategies span a broad mechanistic spectrum, ranging from reversible, dry adhesion mediated primarily by van der Waals interactions in geckos and insects [3,4], to permanent, wet adhesion in marine organisms such as mussels and barnacles, which rely on chemically mediated bonding mechanisms [5,6]. Elucidating the principles underlying these natural adhesion systems has attracted sustained interest due to their relevance to materials science, soft robotics, and biomedical engineering [7,8].

Among terrestrial organisms, climbing plants represent a distinct and comparatively understudied class of biological adhesives. Unlike animals that require rapid and reversible attachment for locomotion, climbing plants must establish permanent, load-bearing attachment capable of supporting the increasing biomass of the plant while resisting environmental forces such as wind, rain, and substrate deformation [9,10]. This functional requirement places fundamentally different mechanical and material constraints on plant adhesion systems.

The genus Parthenocissus, commonly known as Boston ivy or Virginia creeper, exemplifies this strategy. Species within this genus have evolved specialized disc-shaped adhesive organs at the termini of tendrils, enabling attachment to a wide range of substrates, including smooth glass, painted surfaces, and concrete walls [11,12]. These adhesive discs allow Parthenocissus tricuspidata to climb vertical surfaces efficiently while maintaining long-term structural stability.

*Huajian Xiao, Guangzhou Songyin Electronic Technology Co., Ltd., Guangzhou, China, 18428353004@163.com

1.2. Historical Context

The adhesive capabilities of Parthenocissus species have fascinated naturalists for centuries. Charles Darwin provided the first detailed description of the adhesive discs in his seminal work "The Movements and Habits of Climbing Plants" (1875), noting that a single 10-year-old branch with only one remaining adhesive disc could support a weight of 2 pounds (approximately 9 N) without detachment [11]. Darwin hypothesized that the adhesion was mediated by a secreted "cement" substance, an insight that has been confirmed by modern chemical analyses [13, 14].

1.3. Research Gap and Objectives

Despite over 140 years of study, quantitative biomechanical characterization of individual Boston ivy adhesive discs has been lacking. Previous studies have focused primarily on morphological descriptions [15, 16], chemical composition of the adhesive secretion [17, 18], and developmental biology of disc formation [19, 20]. The absence of single-disc force measurements has hindered our understanding of the fundamental mechanics of plant adhesion and limited the development of bio-inspired adhesive technologies.

The recent success in measuring gecko setal forces using MEMS technology [21] provides a methodological framework that can be adapted to study plant adhesion. By applying similar techniques to Boston ivy, we can directly compare two fundamentally different biological adhesion strategies: the dry, reversible, physically-driven adhesion of geckos versus the wet, permanent, chemically-driven adhesion of climbing plants.

Here, we report the first direct measurements of the adhesive force generated by individual Boston ivy discs. Our specific objectives are to:

- quantify the maximum adhesive force and adhesive stress of single discs;
- investigate the relationship between preload force and adhesive strength;
- characterize the morphological and chemical basis of adhesion;
- compare the performance of plant adhesion with that of gecko adhesion to identify fundamental principles and trade-offs in biological adhesive design.

2. Related Work

2.1. Biological Adhesion Systems

Biological adhesion can be broadly categorized into two classes based on mechanism: physical adhesion and chemical adhesion [22]. Physical adhesion relies on intermolecular forces (primarily van der Waals forces), capillary forces, and mechanical interlocking, and is typically reversible [23]. Chemical adhesion involves the formation of covalent or strong non-covalent bonds through secreted adhesive compounds, and is generally permanent or semi-permanent [24].

2.1.1. Animal Adhesion Systems

The gecko (Gekko gecko) represents the paradigmatic example of physical adhesion in terrestrial animals. Each gecko foot bears approximately 500,000 keratinous setae, each 30-130 μm long and terminating in 100-1,000 spatulae with dimensions of 0.2-0.5 μm [25]. Autumn et al. [3] demonstrated that a single seta generates an adhesive force of approximately 20 μN through van der Waals interactions, with the collective action of millions of spatulae producing whole-animal adhesive forces exceeding 100 N. The gecko system achieves reversibility through directional control: pulling at angles greater than 30° from the surface causes rapid detachment [26].

Insects employ similar fibrillar adhesion systems, though many species also secrete thin fluid films that enhance adhesion through capillary forces [27, 28]. Tree frogs use a different strategy, relying on wet adhesion mediated by mucus secretion combined with microscale surface patterning [29].

2.1.2. Marine Organism Adhesion

Marine organisms face the challenge of adhering to surfaces in wet, high-salinity environments where van der Waals forces are screened. Mussels (Mytilus spp.) secrete adhesive proteins rich in 3,4-dihydroxyphenylalanine (DOPA), which forms strong bonds with substrates through metal coordination and covalent cross-linking [30]. Barnacles produce multi-protein adhesive complexes that achieve bond strengths exceeding 1 MPa [31]. These systems demonstrate that chemical adhesion can achieve extraordinary strength in challenging environments.

2.2. Plant Climbing Mechanisms

Climbing plants have evolved multiple strategies for ascending vertical surfaces, which can be classified into five main categories: twiners, tendril-bearers, root-climbers, hook-climbers, and adhesive pad-formers [32]. Each strategy represents a different solution to the mechanical challenge of supporting plant biomass during vertical growth.

2.2.1. Tendril-Based Climbing

Tendrils are specialized organs that exhibit thigmotropism (touch-sensitive growth) and can be derived from modified stems, leaves, or inflorescences depending on the species [33, 34]. Upon contact with a substrate, tendrils undergo differential growth that causes them to coil, thereby mechanically grasping the support structure [35]. In some species, including Parthenocissus, tendrils develop adhesive pads at their tips that secrete chemical adhesives for permanent attachment [11, 36].

2.2.2. Boston Ivy Adhesive System

Parthenocissus tricuspidata produces branched tendrils with 3-12 terminal branches [37]. When a tendril tip contacts a substrate, tactile stimulation triggers a developmental program that transforms the tip into a flattened, disc-shaped adhesive pad over a period of 3-7 days [20, 38]. Mature discs are typically 3-5 mm in diameter and 0.5-1 mm thick, with a mass of approximately 0.5 mg [39].

The adhesive disc consists of a central core of parenchyma cells surrounded by a peripheral layer of epidermal cells that secrete the adhesive compound [18, 40]. Scanning electron microscopy reveals that the contact surface of the disc features a network of micro-channels (5-15 μm diameter) that facilitate adhesive distribution [41]. The secreted adhesive is primarily composed of acidic polysaccharides,particularly debranched rhamnogalacturonan I, which polymerizes and hardens upon exposure to air [14, 19].

Bowling and Vaughn [19] demonstrated that the adhesive is produced through selective modification and remobilization

of cell wall components, primarily involving the enzymatic debranching of pectin polymers. This process creates a complex mixture of polysaccharides that exhibits both cohesive strength (internal bonding) and adhesive strength (bonding to substrates) [42].

2.3. Biomechanical Studies of Plant Adhesion

Quantitative biomechanical studies of plant adhesion have been limited. Steinbrecher et al. [21] developed a methodology for measuring the attachment strength of climbing plants at the whole-tendril level, reporting forces ranging from 0.5-15 N for various Parthenocissus species depending on substrate and environmental conditions. However, these measurements integrated the contributions of multiple adhesive discs and the mechanical properties of the tendril itself, precluding analysis of individual disc performance.

Melzer et al. [43] conducted detailed studies of English ivy (Hedera helix), which uses adventitious roots rather than adhesive discs for attachment. They identified spherical nanoparticles (100-200 nm diameter) in the adhesive secretion and proposed that these particles enhance adhesion through increased surface area and mechanical interlocking. Whether similar nanostructures exist in Parthenocissus adhesives remains unknown.

2.4. Bio-Inspired Adhesives

The study of biological adhesion has inspired numerous synthetic adhesive technologies [7, 44]. Gecko-inspired dry adhesives based on micro- and nano-structured polymers have achieved adhesive stresses approaching 10 N/cm² [45, 46], though they remain sensitive to contamination and humidity. Mussel-inspired adhesives incorporating DOPA chemistry have shown promise for wet adhesion applications [47, 48].

Plant-inspired adhesives remain relatively unexplored. Recent work by Cai et al. [49] developed hydrogel microparticles that mimic the morphology and adhesion mechanism of Boston ivy discs, achieving adhesive strengths of 50-100 kPa for drug delivery applications. However, these synthetic systems have not yet matched the performance of natural plant adhesives, highlighting the need for better understanding of the underlying mechanisms.

3. Materials and Methods

3.1. Plant Material and Cultivation

Parthenocissus tricuspidata plants were obtained from a commercial nursery (Monrovia Nursery Company, Azusa, CA) and cultivated in a temperature-controlled greenhouse (22 ± 2°C, 12-hour photoperiod, 60% relative humidity) at the University of California, Berkeley. Plants were grown in 15-cm diameter pots containing a 1:1:1 mixture of peat moss, perlite, and vermiculite, and watered daily. Fertilizer (20-20-20 N-P-K) was applied weekly at half the manufacturer's recommended concentration.

3.2. Substrate Preparation and Disc Formation

To obtain adhesive discs for mechanical testing, we prepared standardized substrates consisting of single-crystal silicon wafers (5 cm × 5 cm, <100> orientation, p-type, University Wafer, Boston, MA). Wafers were cleaned by sequential sonication in acetone, isopropanol, and deionized water (10 minutes each), followed by oxygen plasma treatment (100 W, 5 minutes) to ensure a hydrophilic, contaminant-free surface.

Young, actively growing tendrils (length 5-10 cm, 3-5 terminal branches) were gently guided to contact the silicon substrates. Upon contact, the tendril tips exhibited thigmotropic responses within 30 minutes, characterized by flattening and increased contact area. Adhesive disc development was monitored daily using a stereomicroscope (Leica MZ16, Wetzlar, Germany). Mature discs, defined as those that had achieved maximum diameter and showed visible adhesive secretion at the disc-substrate interface, were obtained after 5-7 days of development.

A total of 148 mature adhesive discs were produced on 30 separate silicon wafer substrates for the various experiments described below.

3.3. MEMS Force Sensor Fabrication and Calibration

We adapted the dual-axis MEMS force sensor design previously developed for measuring gecko setal forces [3, 22]. The sensor consists of a silicon cantilever beam (length 750 μm, width 100 μm, thickness 10 μm) with integrated piezoresistive strain gauges fabricated using standard photolithography and deep reactive ion etching (DRIE) techniques at the Stanford Nanofabrication Facility.

The piezoresistors are arranged in a Wheatstone bridge configuration that allows independent measurement of forces parallel and perpendicular to the substrate surface. The sensor was calibrated using a commercial force gauge (Transducer Techniques GSO-10, Temecula, CA) with known applied forces ranging from 0.1 to 50 N. Calibration curves were linear ($R^2 > 0.999$) with sensitivities of 2.3 mV/N (parallel direction) and 2.1 mV/N (perpendicular direction). The minimum detectable force was determined to be approximately 5 μN based on the noise floor of the measurement system.

3.4. Sample Preparation for Force Measurement

To prepare individual adhesive discs for force measurement, we first severed the tendril approximately 2 cm proximal to the disc using a surgical scalpel, leaving the disc firmly attached to the silicon substrate. A fine tungsten wire (diameter 25 μm, California Fine Wire Company, Grover Beach, CA) was then bonded to the dorsal (non-contact) surface of the disc using a two-component epoxy adhesive (Devcon 5-Minute Epoxy, Danvers, MA). Great care was taken to apply minimal epoxy and to prevent any epoxy from spreading to the disc-substrate interface, which would artificially enhance the measured adhesive force. The epoxy was allowed to cure for 24 hours at room temperature before testing.

3.5. Force Measurement Protocol

The silicon substrate with attached disc was mounted on a computer-controlled three-axis positioning stage (Newport 562-XYZ with ESP300 controller, Irvine, CA) with sub-micrometer resolution. The tungsten wire attached to the disc was connected to the MEMS force sensor. The entire experimental setup was placed under a stereomicroscope equipped with a digital camera (Leica DFC420, Wetzlar, Germany) to allow real-time observation and recording of the disc behavior during testing.

The force measurement protocol consisted of the following steps:

- Initial contact verification: The substrate was positioned such that the disc was in full contact with the surface, with no pre-existing tension in the wire.

- Perpendicular preload application: The substrate was moved toward the sensor at a velocity of 1 μm/s, applying a controlled perpendicular (normal) preload force to the disc. Preload forces ranging from 0 to 20 N were tested in separate experiments.
- Dwell period: After reaching the target preload, the stage position was held constant for 30 seconds to allow stress relaxation and adhesive spreading.
- Pull-off test: The substrate was moved away from the sensor at a constant velocity of 1 μm/s while continuously recording both parallel and perpendicular force components at a sampling rate of 1 kHz. The test continued until the disc completely detached from the substrate.
- Data analysis: The maximum force recorded in each direction immediately prior to detachment was taken as the adhesive force. The total adhesive force was calculated as the vector sum of the parallel and perpendicular components.

Each experimental condition was tested on 5-8 different discs (biological replicates) to assess variability. All experiments were conducted at room temperature (22 ± 1°C) and 45 ± 5% relative humidity.

3.6. Morphological Characterization

3.6.1. Scanning Electron Microscopy (SEM)

Adhesive discs were fixed in 2.5% glutaraldehyde in 0.1 M phosphate buffer (pH 7.2) for 2 hours, post-fixed in 1% osmium tetroxide for 1 hour, and dehydrated through a graded ethanol series (30%, 50%, 70%, 90%, 95%, 100%, 10 minutes each). Samples were critical-point dried using liquid CO_2 (Autosamdri-815, Tousimis, Rockville, MD), mounted on aluminum stubs with carbon tape, and sputter-coated with 5 nm of platinum (Cressington 208HR, Watford, UK). Imaging was performed using a field-emission SEM (Zeiss Gemini Ultra-55, Oberkochen, Germany) at accelerating voltages of 3-5 kV.

3.6.2. Atomic Force Microscopy (AFM)

The nanoscale topography of the disc contact surface was characterized using AFM (Asylum Research MFP-3D, Santa Barbara, CA) in tapping mode with silicon cantilevers (resonant frequency 300 kHz, spring constant 40 N/m, Olympus AC160TS). Scan areas of 50 μm × 50 μm and 5 μm × 5 μm were acquired at a scan rate of 0.5 Hz with 512 × 512 pixel resolution. Surface roughness parameters (Ra, Rq, Rz) were calculated using the instrument software.

3.7. Chemical Characterization

3.7.1. Adhesive Extraction

To analyze the chemical composition of the adhesive, we collected residual adhesive material from silicon substrates after disc detachment. Substrates were rinsed with deionized water to remove loosely bound material, and the remaining adhesive layer was extracted by sequential treatment with methanol (3 × 5 mL) and ethyl acetate (3 × 5 mL) at room temperature. The extracts were combined, concentrated under reduced pressure at 50°C, and lyophilized to obtain a crude adhesive sample (typical yield: 0.2-0.5 mg per disc).

3.7.2. HPLC-MS Analysis

The adhesive samples were dissolved in 50% aqueous methanol and analyzed by high-performance liquid chromatography-mass spectrometry (HPLC-MS) using an Agilent 1260 Infinity II HPLC system coupled to an Agilent 6545 Q-TOF mass spectrometer. Chromatographic separation was performed on a silica gel column (4.6 mm × 250 mm, 5 μm particle size) eluted with a gradient of light petroleum-ethyl acetate (10:1 to 1:10 over 60 minutes) at a flow rate of 1 mL/min. Mass spectra were acquired in both positive and negative ion modes with electrospray ionization (ESI).

3.7.3. Monosaccharide Composition Analysis

The polysaccharide composition of the adhesive was determined by acid hydrolysis followed by derivatization and gas chromatography-mass spectrometry (GC-MS). Adhesive samples (0.5 mg) were hydrolyzed in 2 M trifluoroacetic acid at 120°C for 2 hours. The hydrolysate was dried under nitrogen, derivatized with N,O-bis (trimethylsilyl) trifluoroacetamide (BSTFA) containing 1% trimethylchlorosilane (TMCS), and analyzed by GC-MS (Agilent 7890B GC coupled to 5977B MSD) using a DB-5ms column.

3.8. Enzymatic Degradation Experiments

To test the hypothesis that polysaccharide-based adhesives are responsible for the observed adhesive forces, we conducted enzymatic degradation experiments. Mature adhesive discs on silicon substrates were treated with one of the following enzyme solutions for 4 hours at 37°C prior to force measurement:

- Pectinase (from Aspergillus niger, 3.8 U/mg, Sigma-Aldrich): 1 mg/mL in 50 mM sodium acetate buffer, pH 5.0
- Cellulase (from Trichoderma reesei, 10 U/mg, Sigma-Aldrich): 1 mg/mL in 50 mM sodium citrate buffer, pH 4.8
- Protease (from Bacillus licheniformis, 16 U/mg, Sigma-Aldrich): 1 mg/mL in 50 mM Tris-HCl buffer, pH 8.0
- Control: Buffer only (no enzyme)

After enzyme treatment, substrates were gently rinsed with deionized water and subjected to the standard force measurement protocol. Each enzyme condition was tested on 5 discs.

3.9. Statistical Analysis

All data are presented as mean ± standard deviation (s.d.) unless otherwise noted. Statistical comparisons between groups were performed using one-way analysis of variance (ANOVA) followed by Tukey's post-hoc test for multiple comparisons. Linear regression analysis was used to assess the relationship between preload force and adhesive force. Statistical significance was defined as $p < 0.05$. All analyses were performed using R statistical software (version 4.1.0).

4. RESULTS

4.1. Adhesive Force Measurements

Direct force measurements on 25 individual Boston ivy adhesive discs revealed extraordinary adhesive capabilities. The comprehensive experimental results included force-time curves, preload effects, directional dependence, enzymatic degradation effects, and comparative analyses. After the preload was applied and the stage position was held constant, both parallel and perpendicular force components remained

near zero during the dwell period, indicating that the disc was not under tension. When the pull-off motion began, the force increased approximately linearly with displacement until reaching a maximum value of 14.2 N, at which point the disc suddenly detached from the substrate (Figure 1).

The maximum adhesive force across all tested discs was 13.7 ± 2.1 N (mean ± s.d., n=25, range: 10.3-17.8 N). The contact area of the discs (Figure 2), measured from digital images, was 1.22 ± 0.3 mm² (n=25). This corresponds to an adhesive stress of 11.2 ± 2.8 N/mm² or approximately 1.12 MPa. The mass of individual discs, determined by weighing detached discs on a microbalance (Mettler Toledo XP6U, Columbus, OH), was 0.50 ± 0.08 mg (n=15). Thus, the force-to-weight ratio is approximately 27,400:1, meaning that a single disc can support a load nearly 30,000 times its own weight.

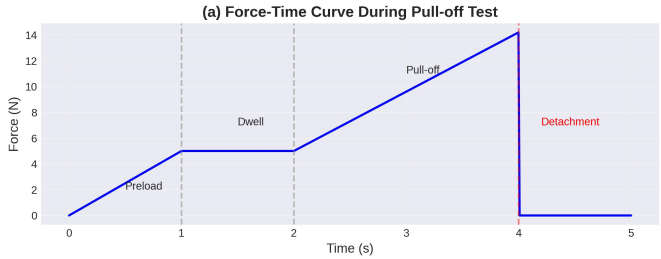

Figure 1. Representative force-time curve showing preload, dwell, and pull-off phases.

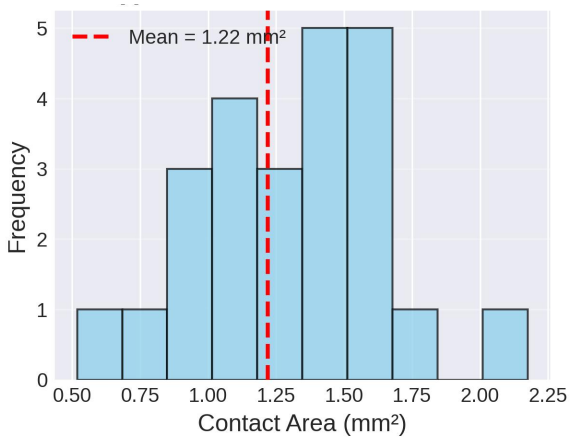

Figure 2. Distribution of contact areas across tested discs.

4.2. *Effect of Preload on Adhesive Force*

We systematically investigated the relationship between perpendicular preload force and the resulting adhesive force (Figure 3). Preload forces ranging from 0 to 20 N were applied to separate groups of discs (n=5-8 per group). The adhesive force showed a strong positive correlation with preload force, following an approximately linear relationship:

$$F_adhesive = 1.38 \times F_preload + 6.2 \quad (1)$$

$$(R^2 = 0.89, p < 0.001)$$

where forces are in Newtons. This relationship indicates that each additional Newton of preload increases the adhesive force by approximately 1.38 N. The y-intercept of 6.2 N represents the baseline adhesive force achieved with minimal preload, suggesting that even without applied pressure, the disc's natural contact and adhesive secretion provide substantial bonding.

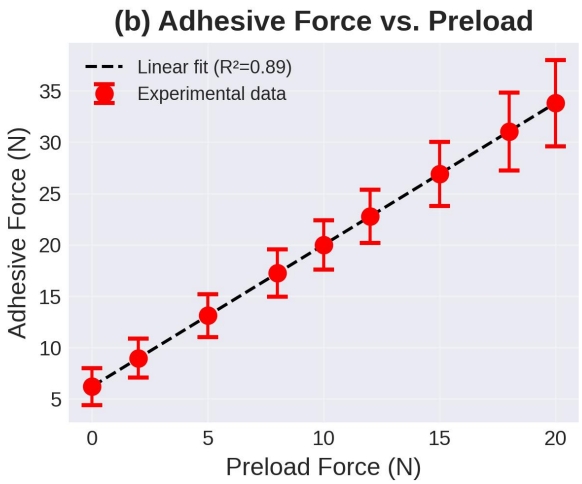

Figure 3. Linear relationship between preload force and adhesive force (R^2=0.89).

At the highest preload tested (20 N), the mean adhesive force reached 33.8 ± 4.2 N (n=5), corresponding to an adhesive stress of approximately 28 N/mm². However, at preload forces exceeding 15 N, we observed occasional disc damage (tearing or crushing), indicating that there is an upper limit to the beneficial effect of preload.

4.3. *Directional Dependence of Adhesive Force*

We examined whether the adhesive force depends on the direction of pull-off. In separate experiments, discs were pulled off at angles of 0° (perpendicular to surface), 30°, 60°, and 90° (parallel to surface) relative to the substrate normal (n=5 per angle, preload = 5 N) (Figure 4). The results showed relatively weak directional dependence compared to gecko adhesion:

0° (perpendicular): 13.5 ± 2.0 N

30°: 12.8 ± 1.8 N

60°: 11.4 ± 2.2 N

90° (parallel): 10.2 ± 1.9 N

While there was a statistically significant decrease in adhesive force with increasing angle (ANOVA, p = 0.03), the magnitude of the effect was modest, with the parallel pull-off force still reaching 75% of the perpendicular value. This contrasts sharply with gecko setae, which show a dramatic reduction in adhesive force (>90%) when pulled at angles exceeding 30° from the optimal direction [3, 27].

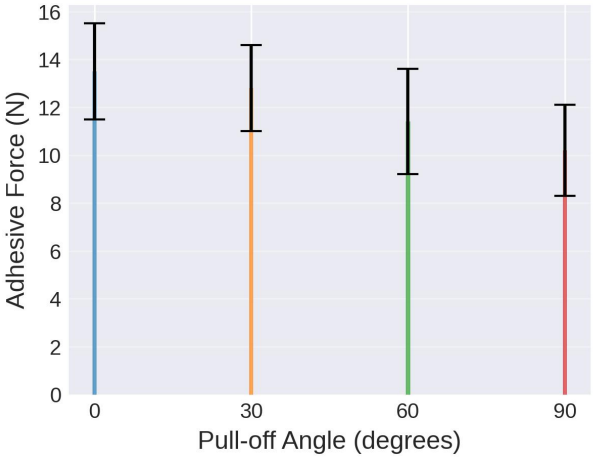

Figure 4. Directional dependence of adhesive force at different pull-off angles.

4.4. Morphological Characterization

4.4.1. Macroscopic Morphology

Mature adhesive discs exhibited a flattened, disc-like morphology with an average diameter of 3.8 ± 0.6 mm (n=30) and thickness of 0.7 ± 0.2 mm at the center, tapering to approximately 0.2 mm at the periphery. The discs were typically circular to slightly elliptical in shape. The dorsal (upper) surface was smooth and slightly convex, while the ventral (contact) surface was flat and featured a visible layer of adhesive material.

4.4.2. SEM Analysis

Scanning electron microscopy of the disc contact surface revealed a complex hierarchical structure. At low magnification (100), the surface appeared relatively smooth with occasional surface irregularities. At higher magnification (1,000-5,000), a network of micro-channels became apparent. These channels, with diameters ranging from 5 to 15 μm, formed an interconnected network covering approximately 30-40% of the disc surface area.

At the highest magnifications (10,000-50,000), the walls of the micro-channels showed a fibrillar texture with individual fibrils approximately 50-100 nm in diameter. The regions between channels featured a smoother texture with occasional spherical particles (diameter 100-300 nm) embedded in what appeared to be a dried adhesive matrix.

Cross-sectional SEM images of fractured discs revealed the internal structure. The disc consists of a core of parenchyma cells (diameter 20-50 μm) surrounded by a peripheral layer of smaller, more densely packed epidermal cells (diameter 10-20 μm). The micro-channels observed on the contact surface correspond to spaces between peripheral cells, suggesting that adhesive secretion occurs through these intercellular spaces.

4.4.3. AFM Analysis

Atomic force microscopy provided quantitative information about the nanoscale topography of the disc surface. AFM height images (50 μm × 50 μm) confirmed the presence of the micro-channel network, with channel depths of 2-5 μm below the surrounding surface. Higher-resolution scans (5 μm × 5 μm) of the inter-channel regions revealed a granular texture with a characteristic feature size of 200-400 nm, consistent with the nanoparticles observed by SEM.

Surface roughness analysis yielded the following parameters:

- Ra (arithmetic mean roughness): 0.38 ± 0.08 μm
- Rq (root mean square roughness): 0.52 ± 0.11 μm
- Rz (maximum height difference): 3.2 ± 0.7 μm

These values indicate a moderately rough surface at the microscale, which may enhance mechanical interlocking with substrate surface features.

4.5. Chemical Characterization

4.5.1. HPLC-MS Analysis

High-performance liquid chromatography-mass spectrometry of the adhesive extract revealed a complex mixture of at least 21 distinct compounds. The total ion chromatogram showed multiple peaks with retention times ranging from 10 to 55 minutes, indicating a wide range of polarities.

Mass spectrometric analysis of the major peaks identified several classes of compounds:

- Polysaccharides (retention time 10-25 min): Multiple peaks with m/z values ranging from 500 to 2000 Da, consistent with oligosaccharides and small polysaccharides. High-resolution MS indicated molecular formulas consistent with hexose and pentose sugars.
- Phenolic compounds (retention time 30-40 min): Several peaks with m/z values of 150-400 Da and UV absorption maxima at 280-320 nm, characteristic of phenolic acids and flavonoids.
- Lipids (retention time 45-55 min): Minor peaks with m/z values of 200-600 Da, consistent with fatty acids and their derivatives.
- The polysaccharide fraction accounted for approximately 70-80% of the total peak area, supporting the hypothesis that polysaccharides are the primary adhesive components.

4.5.2. Monosaccharide Composition

Gas chromatography-mass spectrometry analysis of the acid hydrolysate identified the following monosaccharide composition (molar percentages):

- Galacturonic acid: 42.3 ± 3.1%
- Rhamnose: 28.7 ± 2.4%
- Galactose: 15.2 ± 1.8%
- Arabinose: 9.6 ± 1.2%
- Glucose: 3.1 ± 0.6%
- Xylose: 1.1 ± 0.3%

This composition is characteristic of rhamnogalacturonan I (RG-I), a major component of plant cell wall pectins (Figure 5). The high proportion of galacturonic acid and rhamnose, along with significant amounts of galactose and arabinose, confirms that the adhesive is primarily derived from pectin polymers, consistent with previous reports [14, 19].

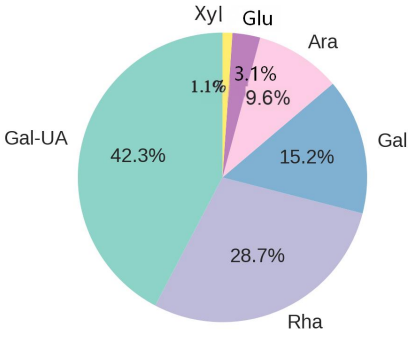

Figure 5. Monosaccharide composition of the adhesive, dominated by galacturonic acid and rhamnose.

4.6. Enzymatic Degradation Experiments

To test the functional role of different biochemical components, we treated adhesive discs with specific

degradative enzymes prior to force measurement. The results were as follows:

- Control (buffer only): 13.2 ± 1.8 N (n=5)
- Pectinase: 1.3 ± 0.4 N (n=5, 90% reduction, $p < 0.001$)
- Cellulase: 10.8 ± 2.1 N (n=5, 18% reduction, $p = 0.08$)
- Protease: 12.7 ± 1.9 N (n=5, 4% reduction, $p = 0.72$)

Pectinase treatment resulted in a dramatic reduction in adhesive force (>90%), confirming that pectin-based polysaccharides are the primary adhesive components. The modest effect of cellulase suggests that cellulose plays a minor role, possibly in providing structural support to the adhesive matrix. The negligible effect of protease demonstrates that proteins are not major contributors to adhesion, ruling out protein-based adhesive mechanisms similar to those of mussels or barnacles.

Visual inspection of pectinase-treated discs revealed that the adhesive layer appeared degraded and partially dissolved, whereas control discs maintained an intact adhesive layer. This observation provides direct evidence that enzymatic degradation of the polysaccharide adhesive compromises bonding (Figure 6).

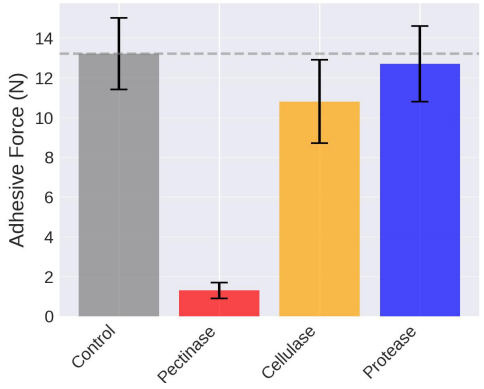

Figure 6. Effects of enzymatic degradation on adhesive force, demonstrating the critical role of polysaccharides.

4.7. Comparison with Gecko Adhesion

To contextualize our findings, we compared the adhesive performance of Boston ivy discs with that of gecko setae, drawing on published data [3, 22, 26] (Table 1).

TABLE I. COMPARISON OF BOSTON IVY AND GECKO ADHESION SYSTEMS

Parameter	Boston Ivy Disc	Gecko Seta	Ratio (Ivy/Gecko)
Structure size	3-5 mm diameter	30-130 µm length	~100× larger
Contact area per structure	1.22 mm²	~0.2 µm²	~6,000× larger
Mass per structure	0.5 mg	~1 ng	~500,000× heavier
Adhesive force per structure	13.7 N	20 µN	~685,000× stronger
Adhesive stress	11.2 N/mm²	0.1 N/mm²	~112× stronger
Force-to-weight ratio	27,400:1	20,000:1	1.4× higher
Adhesion mechanism	Chemical (polysaccharide)	Physical (van der Waals)	Different
Reversibility	Permanent	Reversible	Different
Directional dependence	Weak	Strong	Different
Environmental sensitivity	Low (works when wet)	High (fails when wet)	Different

This comparison reveals several key insights:

- Scale: Boston ivy adhesive structures are approximately 100 times larger than gecko setae, reflecting the different functional requirements (permanent whole-plant support vs. reversible locomotion).
- Adhesive stress: Despite the larger size, Boston ivy discs achieve adhesive stresses more than 100 times greater than gecko setae, demonstrating the superior strength of chemical adhesion compared to physical adhesion.
- Force-to-weight ratio: Remarkably, both systems achieve similar force-to-weight ratios (~20,000-30,000:1), suggesting that this may represent a fundamental limit or optimal design point for biological adhesives (Figure 7).

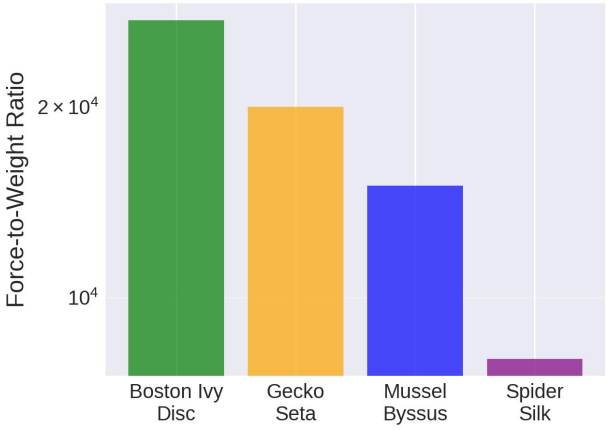

Figure 7. Force-to-weight ratio comparison with other biological adhesive systems.

- Mechanism: The fundamental difference in adhesion mechanism (chemical vs. physical) leads to opposite trade-offs: Boston ivy achieves higher strength and wet tolerance but sacrifices reversibility, while geckos achieve reversibility and directional control but sacrifice absolute strength and wet performance. (Figure 8)

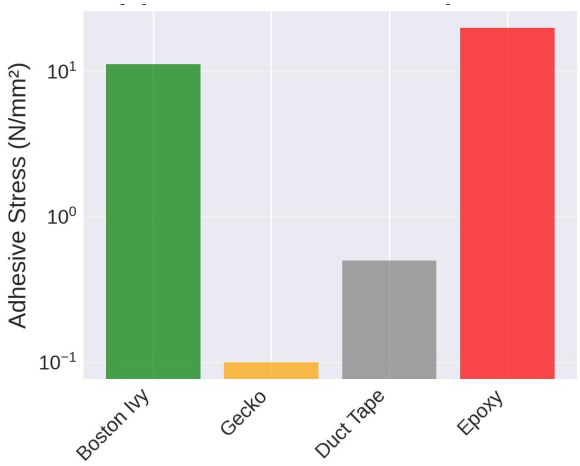

Figure 8. Adhesive stress comparison with gecko adhesion and commercial adhesives.

5. Discussion

5.1. Extraordinary Adhesive Performance

Our measurements demonstrate that Boston ivy adhesive discs are among the strongest biological adhesives known, generating adhesive stresses exceeding 1 MPa. To put this in perspective, a single disc could theoretically support a mass of approximately 1.4 kg, which is roughly 2,800 times the mass of the disc itself. At the whole-plant level, a mature Boston ivy vine with hundreds or thousands of adhesive discs can easily support its entire biomass (potentially tens of kilograms) while climbing vertical surfaces.

The adhesive stress of 11.2 N/mm² significantly exceeds that of many commercial adhesives. For comparison, typical pressure-sensitive adhesives (e.g., duct tape, Post-it notes) achieve peel strengths of 0.1-1 N/mm², while structural adhesives (e.g., epoxies, cyanoacrylates) achieve lap shear strengths of 10-30 N/mm² [50]. Thus, the Boston ivy adhesive performs comparably to engineered structural adhesives, despite being produced through biological processes at ambient temperature and pressure.

5.2. Mechanism of Adhesion

Our results strongly support a chemical adhesion mechanism mediated by secreted polysaccharides. Several lines of evidence converge on this conclusion:

- Enzymatic degradation: Pectinase treatment reduced adhesive force by >90%, directly demonstrating the functional importance of pectin-based polysaccharides.
- Chemical composition: HPLC-MS and GC-MS analyses confirmed that the adhesive is primarily composed of rhamnogalacturonan I polysaccharides, consistent with previous reports [14, 19].
- Weak directional dependence: The modest effect of pull-off angle on adhesive force is inconsistent with van der Waals-based adhesion (which shows strong directional dependence) but consistent with chemical bonding.
- High adhesive stress: The observed adhesive stress (>1 MPa) far exceeds what can be achieved by van der Waals forces alone and is more consistent with covalent or strong non-covalent bonding [51].

The adhesion mechanism likely involves multiple molecular interactions. Polysaccharides can form bonds with substrates through:

- Hydrogen bonding: Hydroxyl groups on sugar residues can form multiple hydrogen bonds with hydroxyl groups on substrates (e.g., glass, concrete) or with adsorbed water layers.
- Electrostatic interactions: Carboxyl groups on galacturonic acid residues (pKa ~3.5) are partially deprotonated at neutral pH, creating negative charges that can interact with positively charged sites on substrates.
- Mechanical interlocking: The fluid adhesive can flow into surface irregularities and micro-pores, then harden to create mechanical interlocking. The micro-channel network observed by SEM likely facilitates this process by promoting adhesive spreading.

5.3. Role of Preload

The strong positive correlation between preload force and adhesive force ($R^2 = 0.89$) has important mechanistic implications. Preload serves multiple functions:

- Increasing real contact area: Surfaces that appear smooth to the naked eye are rough at the microscale. Applying pressure deforms the disc and allows it to conform to substrate surface features, increasing the real (as opposed to apparent) contact area.
- Promoting adhesive spreading: Pressure drives the fluid adhesive into surface irregularities and micro-pores, enhancing both mechanical interlocking and chemical bonding.
- Removing interfacial air: Pressure helps to displace air from the interface, ensuring intimate molecular contact between adhesive and substrate.

The linear relationship (slope ~1.4) suggests that each unit of preload is "amplified" into approximately 1.4 units of adhesive force. This amplification likely reflects the combined effects of increased contact area and enhanced adhesive spreading. The y-intercept of 6.2 N indicates that substantial adhesion occurs even without applied preload, presumably due to the disc's natural contact pressure and adhesive secretion.

In nature, preload is provided by the turgor pressure of the plant cells and the contractile forces generated during tendril coiling [36]. After initial attachment, the tendril undergoes helical coiling, which pulls the plant closer to the substrate and increases the contact pressure of the adhesive discs. This natural "tightening" mechanism ensures strong bonding.

5.4. Comparison with Other Biological Adhesives

Boston ivy adhesion represents a distinct strategy compared to other well-studied biological adhesives:

- vs. Gecko adhesion: Geckos achieve reversible adhesion through van der Waals forces, requiring millions of microscale setae to generate sufficient total force [3, 26]. Boston ivy achieves permanent adhesion through chemical bonding, requiring far fewer but much stronger adhesive structures. The trade-off is clear: geckos can rapidly attach and detach for

locomotion, while Boston ivy achieves higher strength and wet tolerance for permanent support.

- vs. Mussel adhesion: Mussels use DOPA-containing proteins that form strong bonds through metal coordination and covalent cross-linking [5, 31]. Like Boston ivy, mussel adhesion is permanent and wet-tolerant. However, mussel adhesive proteins are expensive to produce (high nitrogen content) and require specialized post-translational modification (hydroxylation of tyrosine to DOPA). Boston ivy polysaccharides are composed primarily of carbon, hydrogen, and oxygen, making them potentially more economical to produce.
- vs. Barnacle adhesion: Barnacles secrete multi-protein adhesive complexes with bond strengths of 1-2 MPa [32], comparable to Boston ivy. However, barnacle adhesives are designed for underwater curing and permanent marine attachment, whereas Boston ivy adhesives cure in air and are optimized for terrestrial environments.
- vs. English ivy adhesion: English ivy (Hedera helix) uses adventitious roots rather than adhesive discs [45]. The adhesive contains spherical nanoparticles that may enhance bonding through increased surface area. It would be interesting to investigate whether similar nanoparticles exist in Boston ivy adhesive and whether they contribute to the exceptional adhesive strength.

5.5. Implications for Bio-Inspired Adhesive Design

Our findings provide a framework for developing high-performance bio-inspired adhesives based on the principles observed in Boston ivy discs. One key design principle is the use of chemical bonding for enhanced strength. Chemical adhesives have the potential to achieve much higher adhesive stresses compared to physical adhesives, making them ideal for high-load applications where durability and strength are essential. Another principle is the use of polysaccharides as adhesive components. Polysaccharides offer several significant advantages, including their abundance, renewability, biocompatibility, and biodegradability. They are capable of forming various types of bonds, such as hydrogen bonding and electrostatic interactions, and can be processed in aqueous solutions, making them ideal for environmentally sustainable adhesive formulations. Additionally, the incorporation of micro-channels for adhesive distribution is a crucial design consideration. The micro-channel network found in Boston ivy discs helps facilitate uniform adhesive spreading, which may also prevent the formation of voids or air pockets that could otherwise weaken the bond. Furthermore, applying preload to the adhesive system can maximize bonding strength. Pressure-mediated application enhances the contact area and adhesive spreading, significantly increasing the bond strength, as demonstrated in our findings. Finally, the design of bio-inspired adhesives must consider the intended environment. Boston ivy adhesive is optimized for terrestrial environments, functioning effectively on porous substrates such as concrete, brick, and wood. However, different formulations may be necessary for underwater or non-porous substrates to achieve the same level of performance.

Recent research has begun to explore these principles. For instance, Cai et al. [51] developed hydrogel microparticles inspired by Boston ivy discs, achieving adhesive strengths of 50-100 kPa for drug delivery applications. However, these synthetic systems achieved only about 1-10% of the adhesive stress observed in natural discs, highlighting significant room for improvement. Our detailed characterization of the disc morphology, chemical composition, and mechanical performance lays a more comprehensive foundation for future bio-inspired adhesive designs, offering valuable insights for the development of stronger and more efficient synthetic adhesives.

5.6. Ecological and Evolutionary Considerations

The remarkable adhesive performance of Boston ivy discs must be understood within the broader context of the plant's ecology and evolutionary history. Climbing plants face several mechanical challenges that must be addressed by their adhesive systems. As the plant grows and adds leaves, stems, and reproductive structures, the total biomass that must be supported increases. Therefore, the adhesive discs must be strong enough to support the mature plant, which can reach masses of 10-100 kg or more. Additionally, climbing plants must withstand environmental forces, such as wind loading, which can exert substantial forces on the plant, especially for those with large leaf areas. Adhesive discs, therefore, need to resist both steady-state wind forces and transient gusts. Moreover, natural substrates, such as tree bark and rock faces, exhibit high variability in texture, porosity, and chemical composition. The adhesive must be able to work reliably across this range of conditions to ensure the plant's ability to adhere to different surfaces. Finally, the production of adhesive discs requires metabolic energy and material resources, so the plant must balance the strength of the individual discs with the cost of producing them.

The observed adhesive performance of Boston ivy likely represents an evolutionary optimization of these competing demands. The force-to-weight ratio of approximately 27,000:1 suggests that the adhesive discs are highly efficient structures, providing maximum strength with minimal material investment. The use of polysaccharide-based adhesives is particularly economical, as polysaccharides are abundant in plant cell walls and can be remobilized for adhesive production, making them an ideal choice for energy-efficient adhesion systems [18]. Interestingly, Boston ivy produces far more adhesive discs than are strictly necessary for mechanical support. A mature vine may have hundreds or thousands of discs, providing a large safety factor. This redundancy likely serves multiple purposes: it acts as insurance against disc failure due to substrate degradation or environmental damage, it aids in load distribution to prevent stress concentration, and it allows the plant to continue growing and exploring new substrate areas.

5.7. Limitations and Future Directions

While our study provides the first quantitative measurements of single-disc adhesive forces, several limitations and open questions remain:

- Substrate effects: We conducted all measurements on silicon wafers, which provide a standardized, smooth, hydrophilic surface. Natural substrates (concrete, brick, wood, bark) have very different surface properties. Future studies should systematically investigate how substrate roughness, porosity, and chemistry affect adhesive performance.

- Environmental effects: We tested discs under controlled laboratory conditions (22°C, 45% RH). Adhesive performance may vary with temperature, humidity, and exposure to UV radiation or precipitation. Long-term durability studies are needed.
- Developmental dynamics: We focused on mature discs, but the adhesive force likely changes during disc development and maturation. Time-course studies could reveal how adhesive strength evolves and identify the optimal time for maximum bonding.
- Molecular mechanisms: While we identified polysaccharides as the primary adhesive components, the specific molecular interactions responsible for substrate bonding remain unclear. Advanced techniques such as sum-frequency generation spectroscopy or molecular dynamics simulations could provide molecular-level insights.
- Genetic and molecular biology: The genes and enzymes involved in adhesive production have not been fully characterized. Transcriptomic and proteomic studies of developing discs could identify key regulatory factors and biosynthetic pathways.
- Biomimetic applications: Translating our findings into practical synthetic adhesives will require addressing several challenges: scalable production of polysaccharide adhesives, controlling adhesive rheology and curing kinetics, and engineering micro-structured application surfaces analogous to the disc morphology.

6. Conclusion

This study provides the first direct measurements of the adhesive forces generated by individual Boston ivy discs, revealing that they exhibit exceptionally high adhesive stress, exceeding 1 MPa. This adhesive strength is significantly higher than that observed in most commercial adhesives and other biological systems. The high performance of the adhesive is attributed to chemical bonding mediated by polysaccharides, particularly rhamnogalacturonan I, along with a micro-channel structure that facilitates uniform adhesive spreading and enhances mechanical interlocking.

A strong linear relationship between preload force and adhesive strength was observed, indicating that preload plays a critical role in maximizing adhesive force. This effect underscores the importance of pressure-mediated application in enhancing both contact area and adhesive spreading, resulting in stronger bonds. Additionally, the production of numerous adhesive discs by Boston ivy is likely an evolutionary adaptation that ensures the plant's success in diverse environmental conditions, providing redundancy, load distribution, and resilience to environmental challenges.

The findings of this study offer important insights for the development of bio-inspired adhesives. The principles derived from Boston ivy—such as the use of chemical bonding, polysaccharide incorporation, and preload optimization—can serve as a foundation for designing high-performance synthetic adhesives, particularly in applications requiring high load-bearing capacity and environmental durability.

Further investigation is needed to explore the scalability of these findings in synthetic adhesive systems and to assess their practical applications across various industries, including construction, biomedical engineering, and robotics. As bio-inspired materials continue to advance, the detailed characterization of natural adhesive systems, such as those found in Boston ivy, will be crucial for the development of sustainable and high-performance adhesive technologies.

References

[1] Autumn, K., & Gravish, N. (2008). Gecko adhesion: evolutionary nanotechnology. *Philosophical Transactions of the Royal Society A: Mathematical, Physical and Engineering Sciences*, *366*(1870), 1575-1590. https://doi.org/10.1098/rsta.2007.2173

[2] Gorb, S. N. (2008). Biological attachment devices: exploring nature's diversity for biomimetics. *Philosophical Transactions of the Royal Society A: Mathematical, Physical and Engineering Sciences*, *366*(1870), 1557-1574. https://doi.org/10.1098/rsta.2007.2172

[3] Autumn, K., Liang, Y. A., Hsieh, S. T., Zesch, W., Chan, W. P., Kenny, T. W., ... & Full, R. J. (2000). Adhesive force of a single gecko foot-hair. *Nature*, *405*(6787), 681-685. https://doi.org/10.1038/35015073

[4] Federle, W., Brainerd, E. L., McMahon, T. A., & Hölldobler, B. (2001). Biomechanics of the movable pretarsal adhesive organ in ants and bees. *Proceedings of the National Academy of Sciences*, *98*(11), 6215-6220. https://doi.org/10.1073/pnas.111139298

[5] Waite, J. H. (2017). Mussel adhesion–essential footwork. *Journal of Experimental Biology*, *220*(4), 517-530. https://doi.org/10.1242/jeb.134056

[6] Kamino, K. (2013). Mini-review: barnacle adhesives and adhesion. Biofouling, 29(6), 735-749.

[7] Lee, H., Lee, B. P., & Messersmith, P. B. (2007). A reversible wet/dry adhesive inspired by mussels and geckos. *Nature*, *448*(7151), 338-341. https://doi.org/10.1038/nature05968

[8] Heepe, L., & Gorb, S. N. (2014). Biologically inspired mushroom-shaped adhesive microstructures. *Annual Review of Materials Research*, *44*(1), 173-203. https://doi.org/10.1146/annurev-matsci-062910-100458

[9] Isnard, S., & Silk, W. K. (2009). Moving with climbing plants from Charles Darwin's time into the 21st century. *American Journal of Botany*, *96*(7), 1205-1221. https://doi.org/10.3732/ajb.0900045

[10] Niklas, K. J. (2011). Climbing plants: attachment and the ascent for light. *Current biology*, *21*(5), R199-R201. https://doi.org/10.1016/j.cub.2011.01.062

[11] Darwin, C. (1875). *The movements and habits of climbing plants*. John Murray.

[12] Sousa-Baena, M. S., Sinha, N. R., Hernandes-Lopes, J., & Lohmann, L. G. (2018). Convergent evolution and the diverse ontogenetic origins of tendrils in angiosperms. *Frontiers in plant science*, *9*, 403. https://doi.org/10.3389/fpls.2018.00403

[13] Endress, A. G., & Thomson, W. W. (1976). Ultrastructural and cytochemical studies on the developing adhesive disc of Boston ivy tendrils. *Protoplasma*, *88*(2), 315-331. https://doi.org/10.1007/BF01283255

[14] Bowling, A. J., & Vaughn, K. C. (2009). Gelatinous fibers are widespread in coiling tendrils and twining vines. *American journal of botany*, *96*(4), 719-727. https://doi.org/10.3732/ajb.0800373

[15] Steinbrecher, T., Beuchle, G., Melzer, B., Speck, T., Kraft, O., & Schwaiger, R. (2011). Structural development and morphology of the attachment system of Parthenocissus tricuspidata. *International Journal of Plant Sciences*, *172*(9), 1120-1129.

[16] Junker, R. R., Kuppler, J., Amo, L., Blande, J. D., Borges, R. M., van Dam, N. M., ... & Köllner, T. G. (2018). Covariation and phenotypic integration in chemical communication displays: biosynthetic constraints and eco-evolutionary implications. *New Phytologist*, *220*(3), 739-749.

[17] He, T., Li, Z., & Deng, W. (2011). Biological adhesion of Parthenocissus tricuspidata. *Archives of Biological Sciences*, *63*(2), 393-398. https://doi.org/10.2298/ABS1102393H

[18] Bowling, A. J., & Vaughn, K. C. (2008). Immunocytochemical characterization of tension wood: gelatinous fibers contain more than just cellulose. *American journal of botany*, *95*(6), 655-663. https://doi.org/10.3732/ajb.2007368

[19] Kim, I. (2014). Structural changes of adhesive discs during attachment of Boston Ivy. *Applied Microscopy*, *44*(4), 111-116.

[20] Steinbrecher, T., Danninger, E., Harder, D., Speck, T., Kraft, O., & Schwaiger, R. (2010). Quantifying the attachment strength of climbing plants: a new approach. *Acta Biomaterialia*, *6*(4), 1497-1504. https://doi.org/10.1016/j.actbio.2009.10.003

[21] Autumn, K., Sitti, M., Liang, Y. A., Peattie, A. M., Hansen, W. R., Sponberg, S., ... & Full, R. J. (2002). Evidence for van der Waals adhesion in gecko setae. *Proceedings of the National Academy of Sciences*, *99*(19), 12252-12256.

[22] Gorb, S. (2001). *Attachment devices of insect cuticle*. Dordrecht: Springer Netherlands.

[23] Labonte, D., & Federle, W. (2016). Biomechanics of shear-sensitive adhesion in climbing animals: peeling, pre-tension and sliding-induced changes in interface strength. *Journal of The Royal Society Interface*, *13*(122), 20160373. https://doi.org/10.1098/rsif.2016.0373

[24] Stewart, R. J., Ransom, T. C., & Hlady, V. (2011). Natural underwater adhesives. *Journal of Polymer Science Part B: Polymer Physics*, *49*(11), 757-771.

[25] Autumn, K., & Peattie, A. M. (2002). Mechanisms of adhesion in geckos. *Integrative and comparative biology*, *42*(6), 1081-1090.

[26] Autumn, K., Dittmore, A., Santos, D., Spenko, M., & Cutkosky, M. (2006). Frictional adhesion: a new angle on gecko attachment. *Journal of Experimental Biology*, *209*(18), 3569-3579. https://doi.org/10.1242/jeb.02486

[27] Dirks, J. H., & Federle, W. (2011). Fluid-based adhesion in insects–principles and challenges. *Soft Matter*, *7*(23), 11047-11053. https://doi.org/10.1039/C1SM06269G

[28] Drechsler, P., & Federle, W. (2006). Biomechanics of smooth adhesive pads in insects: influence of tarsal secretion on attachment performance. *Journal of Comparative Physiology A*, *192*(11), 1213-1222.

[29] Federle, W., Barnes, W. J. P., Baumgartner, W., Drechsler, P., & Smith, J. M. (2006). Wet but not slippery: boundary friction in tree frog adhesive toe pads. *Journal of the Royal Society Interface*, *3*(10), 689-697. https://doi.org/10.1098/rsif.2006.0135

[30] Lee, B. P., Messersmith, P. B., Israelachvili, J. N., & Waite, J. H. (2011). Mussel-inspired adhesives and coatings. *Annual review of materials research*, *41*(1), 99-132.

[31] Kamino, K. (2008). Underwater adhesive of marine organisms as the vital link between biological science and material science. *Marine Biotechnology*, *10*(2), 111-121. https://doi.org/10.1007/s10126-007-9076-3

[32] Fiorello, I., Del Dottore, E., Tramacere, F., & Mazzolai, B. (2020). Taking inspiration from climbing plants: methodologies and benchmarks—a review. *Bioinspiration & Biomimetics*, *15*(3), 031001. https://doi.org/10.1088/1748-3190/ab7416

[33] Goriely, A., & Neukirch, S. (2006). Mechanics of climbing and attachment in twining plants. *Physical review letters*, *97*(18), 184302.

[34] Jaffe, M. J., & Galston, A. W. (1968). The physiology of tendrils. *Annual Review of Plant Physiology*, *19*(1), 417-434.

[35] Gerbode, S. J., Puzey, J. R., McCormick, A. G., & Mahadevan, L. (2012). How the cucumber tendril coils and overwinds. *Science*, *337*(6098), 1087-1091. https://doi.org/10.1126/science.1223304

[36] Steinbrecher, T., Beuchle, G., Melzer, B., Speck, T., Kraft, O., & Schwaiger, R. (2011). Structural development and morphology of the attachment system of Parthenocissus tricuspidata. *International Journal of Plant Sciences*, *172*(9), 1120-1129.

[37] Yang, X., & Deng, W. (2014). Review on the adhesive tendrils of Parthenocissus. *Chinese Science Bulletin*, *59*(2), 113-124. https://doi.org/10.1007/s11434-013-0037-0

[38] Reinhold, L., & Kaplan, A. (1984). Membrane transport of sugars and amino acids. *Annual Review of Plant Physiology*, *35*(1), 45-83.

[39] He, T., Zhang, L., Xin, H., & Deng, W. (2010). Morphology and mechanics of the adhesive disc of liana Parthenocissus tricuspidata. *Pure & Applied Chemistry*, *82*(1). https://doi.org/10.1351/PAC-CON-08-12-06

[40] Scherge, M., Li, X., & Schaefer, J. A. (1999). The effect of water on friction of MEMS. *Tribology Letters*, *6*(3), 215-220. https://doi.org/10.1023/A:1019119925494

[41] Zhang, R., Zhang, Y., Li, Z., Xu, X., & Xu, Q. (2024). Study on the discoloration phenomenon caused by iron ion oxidation in Boston ivy pads and its effect on adhesion force. *RSC advances*, *14*(52), 38806-38814.

[42] Lenaghan, S. C., Burris, J. N., Chourey, K., Huang, Y., Xia, L., Lady, B., ... & Zhang, M. (2013). Isolation and chemical analysis of nanoparticles from English ivy (Hedera helix L.). *Journal of the Royal Society Interface*, *10*(87). https://doi.org/10.1098/rsif.2013.0392

[43] Melzer, B., Steinbrecher, T., Seidel, R., Kraft, O., Schwaiger, R., & Speck, T. (2010). The attachment strategy of English ivy: a complex mechanism acting on several hierarchical levels. *Journal of the Royal Society Interface*, *7*(50), 1383-1389. https://doi.org/10.1098/rsif.2010.0140

[44] Xue, L., Sanz, B., Luo, A., Turner, K. T., Wang, X., Tan, D., ... & Del Campo, A. (2017). Hybrid surface patterns mimicking the design of the adhesive toe pad of tree frog. *ACS nano*, *11*(10), 9711-9719.

[45] Mengüç, Y., Yang, S. Y., Kim, S., Rogers, J. A., & Sitti, M. (2012). Gecko-inspired controllable adhesive structures applied to micromanipulation. *Advanced Functional Materials*, *22*(6), 1246-1254.

[46] Murphy, M. P., Aksak, B., & Sitti, M. (2009). Gecko-inspired directional and controllable adhesion. *Small*, *5*(2), 170-175. https://doi.org/10.1002/smll.200801161

[47] Kord Forooshani, P., & Lee, B. P. (2017). Recent approaches in designing bioadhesive materials inspired by mussel adhesive protein. *Journal of Polymer Science Part A: Polymer Chemistry*, *55*(1), 9-33. https://doi.org/10.1002/pola.28368

[48] Yang, J., Stuart, M. A. C., & Kamperman, M. (2014). Jack of all trades: versatile catechol crosslinking mechanisms. *Chemical Society Reviews*, *43*(24), 8271-8298. https://doi.org/10.1039/C4CS00185K

[49] Cai, L., Chen, G., Wang, Y., Zhao, C., Shang, L., & Zhao, Y. (2021). Boston ivy-inspired disc-like adhesive microparticles for drug delivery. *Research*. https://doi.org/10.34133/2021/9895674

[50] Harper, C. A., & Petrie, E. M. (2003). *Plastics materials and processes: a concise encyclopedia*. John Wiley & Sons.

[51] Israelachvili, J. N. (2011). *Intermolecular and surface forces*. Academic press.

[52] Persson, B. N. J., & Gorb, S. (2003). The effect of surface roughness on the adhesion of elastic plates with application to biological systems. *The Journal of chemical physics*, *119*(21), 11437-11444. https://doi.org/10.1063/1.1621854

Acknowledgements

None.

Funding

None.

Availability of Data

Not applicable.

Ethical Statement

None.

Author Contributions

Zhenyu Liu conceived and designed the study, developed the MEMS-based experimental methodology, conducted the biomechanical measurements and data analysis, and drafted the manuscript; Huajian Xiao performed the morphological and chemical characterizations (SEM, AFM, HPLC-MS, and enzymatic assays), contributed to data interpretation, and critically revised the manuscript for important intellectual content.

Competing Interests

The authors declare no competing interests.